Critical behaviour of the random field Ising model

1998 J. Phys. A: Math. Gen. 31 85

(http://iopscience.iop.org/0305-4470/31/1/013)

J. Phys. A: Math. Gen. **31** (1998) 85–105. Printed in the UK PII: S0305-4470(98)84710-0

Critical behaviour of the random field Ising model

J-Y Fortin† and P C W Holdsworth‡

Laboratoire de Physique Théorique ENSLAPP§, ENSLyon, 46 Allée d'Italie, F-69364 Lyon Cedex 07, France

Received 4 June 1997, in final form 24 September 1997

Abstract. We present an analytic real-space renormalization group calculation for the random-field Ising model. We apply the Migdal–Kadanoff approximation for the renormalization of a cubic cell in dimensions d, introducing a new field partitioning scheme which allows us to treat the random-field fluctuations in a coherent manner. Our scheme leads naturally to a lower critical dimensionality $d_l = 2$ and allows us to calculate a complete set of three independent exponents in arbitrary dimension. In three dimensions the magnetization exponent $\beta \approx 0.02$ and the Schwartz–Soffer inequality is almost satisfied as an equality. We expand analytically in $\epsilon = d-2$. Further, we show that β and the magnitude of the inequality go to zero exponentially with $1/\epsilon^2$. We calculate the crossover exponent, ϕ from pure to the random-field system and find surprisingly good agreement with experimental values. We find that ϕ satisfies the Schwartz–Soffer inequality: $\phi \geqslant \gamma_0$, the susceptibility exponent of the pure system. We expand in $\epsilon = d-1$ and find that the magnitude of the inequality varies exponentially in $1/\epsilon$. Finally we find that dimensional reduction is satisfied to first order in ϵ, with the reduced dimension $d' = d/2$.

1. Introduction

The random-field Ising model (RFIM) is one of a number of model disordered systems that has been intensively studied over the last two decades (for reviews see, for example [1–3]). After much confusion a coherent picture of its behaviour is finally emerging.

The model is defined with the Hamiltonian

$$H = -J\sum_{\langle i,j\rangle} S_i S_j - \sum_i h_i S_i \qquad S_i = \pm 1 \tag{1}$$

where J is a ferromagnetic coupling constant ($J > 0$) and h_i is a random field at site i which we take to have a Gaussian distribution

$$P(h_i) = \sqrt{\frac{1}{2\pi h^2}}\exp\left(\frac{(h_i - h_0)^2}{2h^2}\right) \tag{2}$$

with mean value h_0 and variance h. In the following discussion h_0 is taken to be zero.

For a long time the main discussion centred around the value of the lower critical dimension and the very existence of a phase transition in a physically realizable system. The physical argument of Imry and Ma [4] in which the energy of a domain of size L is minimized with respect to the wall energy, varying as L^{d-1}, and the random-field energy varying as $L^{d/2}$, gives $d_l = 2$.

† E-mail address: jyfortin@enslapp.ens-lyon.fr
‡ E-mail address: pcwh@enslapp.ens-lyon.fr
§ URA 14-36 du CNRS, associée à l'ENS de Lyon, et à l'Université de Savoie.

0305-4470/98/010085+21$19.50

Alternatively, a number of calculations based on series expansions of the free energy [5–7] exposed a correspondence between the random field model in dimension d and a pure Ising system in dimension $d-2$. This result, known as 'dimensional reduction', therefore gives $d_l = 3$ and no finite temperature phase transition in three dimensions. This result holds to all orders in the perturbation and appears to be rigorous. It was therefore perhaps surprising to find convincing evidence of a transition from experimental realizations of the RFIM [8] such as the diluted antiferromagnet $Fe_xZn_{1-x}Cl_2$ in magnetic field [9]. Subsequent exact calculations showed that, for weak random fields, a magnetic phase is stable at low temperatures [11, 12]. Numerical work confirmed the similarity between the diluted antiferromagnets and the RFIM [13, 14] and it therefore rapidly became clear that there is indeed a phase transition in three dimensions. Interest then passed, first to explaining why the perturbation calculation is wrong and subsequently onto the details of the transition itself.

An explanation for these conflicting results lies in the apparition of metastable states in the region of the transition and the development of a complex free energy surface for which there is experimental [15], theoretical [16–18] and numerical [13, 19] evidence. Villain [17] and Fisher [18] argued that in the critical region, the domain walls are not free to meander continuously and without constraint over the sample. Rather, the random field disorder constrains the domain walls to particular regions of space giving discrete preferred paths. The discrete paths are separated by free energy barriers, which lead to domain wall pinning, metastable domain wall configurations and exponentially long relaxation times. The starting point for the perturbation calculations assumes a single minimum about which the expansion of the free energy is made. If many minima exist, each should be taken into consideration [17, 20]. The calculation of the correct Boltzmann weights for these minima is not, at present, a feasible problem.

The complex structure of the free energy appears therefore to stabilize the magnetic phase in three dimensions. It makes it, however, very difficult to measure details of the transition as the exponentially long timescales guarantee loss of ergodicity and non-equilibrium, or glassy behaviour, as one enters the critical region. The same problems arise in numerical work [21], while in theoretical approaches the difficulty is found in averaging correctly over the disorder. Despite these problems there is now a growing body of work offering a coherent picture of the transition. It predicts it to be second order, driven almost first order by the configurational disorder of the random fields.

In this paper we present an analytic real-space renormalization-group calculation using the Migdal–Kadanoff technique which gives further weight to this picture. We present a new series of approximations that allow us to deal with the random-field disorder in a consistent manner, without recourse to the use of replicas. A preliminary account of this work can be found in [22].

On renormalizing the length scale of the problem, the flow, in variables $\tau = 1/K = T/J$ and $\omega = h/J$ are dominated by the 'random-field' or 'zero-temperature' fixed point at $\tau = 0, \omega = \omega_c$, as shown schematically in figure 1. The zero-temperature fixed point is a direct consequence of the metastability: the system becomes frozen by the random fields with the result that the critical fluctuations in the system are due to the configurational disorder of the random fields rather than thermal fluctuations [18]. It is the reason why temperature, T, is an irrelevant variable in the renormalization of the RFIM [24].

Close to the fixed point the renormalization equations for a change of scale b take the form

$$\begin{aligned} &(h_0/T)' = b^x(h_0/T) \qquad \tau' = b^{-y}\tau \qquad \delta\omega' = b^z\delta\omega \\ &\delta\omega = \omega - \omega_c \end{aligned} \tag{3}$$

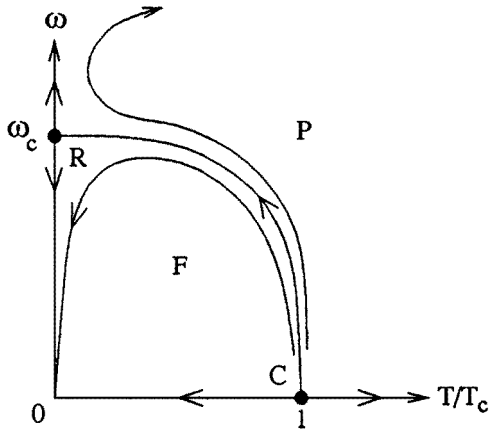

Figure 1. Schematic flow diagram for the RFIM for $d > d_l$. F marks the ferromagnetic phase and P marks the paramagnetic phase.

with x, y and z all positive. At this point the divergent part of the free energy and correlation length should take the form [24]

$$\begin{aligned} E &= Jf(\delta\omega, h_0/J) \\ \xi &= \xi(\delta\omega, h_0/J). \end{aligned} \tag{4}$$

At first sight one might therefore expect just two independent exponents. However, J changes with length scale at the fixed point and therefore x, y, z are all implicated, despite the temperature being irrelevant [23]: the rescaled quantities are

$$\begin{aligned} E' &= Eb^d = b^y Jf(b^z\delta\omega, b^{x-y}h_0/J) \\ \xi' &= \xi b^{-1} = \xi(b^z\delta\omega, b^{x-y}h_0/J). \end{aligned} \tag{5}$$

An open question is therefore: are the three exponents independent? The supplementary exponent results physically from a divergence in the susceptibility which is particular to a zero-temperature fixed point: in reciprocal space, at small wave vector, the susceptibility at the transition has the form

$$\chi(\boldsymbol{q}) = [\langle S_q S_{-q}\rangle - \langle S_q\rangle\langle S_{-q}\rangle] \sim 1/q^{2-\eta} \tag{6}$$

where S_q is a spin at wave vector $\boldsymbol{q}$, $\langle\ldots\rangle$ represents a thermal average, and $[\ldots]$ a configurational average over the disorder. In the pure system, where the driving force is the thermal fluctuations, $\langle S_q\rangle = 0$ at T_C, but here at the zero-temperature fixed point the correlations are frozen in by the disorder and both terms in the expression for the susceptibility are divergent. In fact they are more divergent than the difference between them [2, 23] and one must define a disconnected susceptibility

$$\chi^{\mathrm{dis}}(\boldsymbol{q}) = [\langle S_q\rangle\langle S_{-q}\rangle] \sim 1/q^{4-\overline{\eta}} \tag{7}$$

with exponent $\overline{\eta}$. If η and $\overline{\eta}$ are independent then there is a third exponent which comes from the remnants of thermal fluctuations and temperature plays the role of a dangerously irrelevant variable [25]. Following the scaling relations for the RFIM (section 3), an effective dimension can be defined $d' = d - 2 + \theta = d - y$ with $\theta = \overline{\eta} - \eta$.

One can deduce limits for the value of the third exponent from the exact Schwartz–Soffer inequality [26]: $\overline{\eta} \leqslant 2\eta$ and the result corresponding to dimensional reduction: $\overline{\eta} = \eta$ [27]. These two extremes are therefore both consistent with two-parameter scaling. The

most reliable information concerning quantitative values comes from high-temperature series expansions [28], where to 15th order in $1/T$ ones finds the inequality to hold as an equality, $\overline{\eta} = 2\eta$, indicating that there could, after all, only be two independent exponents. However, this is not entirely consistent with the results of Mézard and Young [27], who investigated the question of replica symmetry breaking. The existence of metastable states and the associated complex free energy brings to mind the multivalley free energy structure of replica symmetry breaking in spin glasses [20]. Within a self-consistent screening approximation and an expansion in $1/m$, where m is the number of spin components ($m = 1$ for the Ising model), they show that the dimensional reduction result $d' = d - 2$, $\overline{\eta} = \eta$ corresponds to a replica-symmetric solution, which is unstable at the transition. They show further that the stable solution has broken replica symmetry and predict $\overline{\eta} - 2\eta < 0$, with values lying in a narrow range close to zero, but which they are unable to calculate. Other methods suggest that [13, 19], as the correlation length diverges, the spin structures pinned by the disorder become macroscopically large, while at the same time the transition rate between them falls to zero [29]. From this one could conclude that the large scale and 'frozen' spin structures, which occur in the region of the transition, translate to true replica symmetry breaking as one approaches T_C.

In the next section we present our one-dimensional decimation procedure and the Migdal–Kadanoff procedure that allows us to move to higher dimension. In section 3 we present our results in three dimensions. We compare our findings, first with other renormalization procedures and then with experimental and numerical results. In section 4 we expand analytically in $\epsilon = d-2$ and find that both $\overline{\eta}-2\eta$ and β tend to zero exponentially with $1/\epsilon^2$. In section 5 we discuss the crossover from pure to random field behaviour for weak disorder and calculate the crossover exponent ϕ in arbitrary dimension. We are able to compare this favourably with experimental results in three dimensions. Finally, we give some discussion of our results in section 6. Further details of the Migdal–Kadanoff procedure can be found in the appendices.

2. Migdal–Kadanoff renormalization

We begin with a decimation procedure for a one-dimensional chain, which we then generalize to dimensions-d using the Migdal–Kadanoff approximation. Throughout we take the microscopic lattice constant to be unity. Evaluating the trace over alternate spins on an N spin chain, the relevant part of the new partition function for an $N/2$ spin chain can be expressed in the form

$$Z_{i-1,i+1} = \delta \exp \beta [J'_{i-1,i+1} S_{i-1} S_{i+1} + h'_{i-1} S_{i-1} + h'_{i+1} S_{i+1}] \tag{8}$$

where $\beta = 1/k_B T$ and δ is a constant. The transformations for $J'_{i-1,i+1}$ and h'_i in terms of the initial variables are given by

$$\begin{aligned}
J'_{i-1,i+1} &= \frac{1}{4\beta} \log \left(\frac{\cosh \beta (J_{i-1,i} + J_{i,i+1} + h_i) \cosh \beta (J_{i-1,i} + J_{i,i+1} - h_i)}{\cosh \beta (-J_{i-1,i} + J_{i,i+1} + h_i) \cosh \beta (J_{i-1,i} - J_{i,i+1} + h_i)} \right) \\
h'_{i+1} &= h_{i+1} + H_{i+1,-1} + H_{i+1,+1} \\
H_{i+1,\sigma} &= \frac{1}{4\beta} \log \left(\frac{\cosh \beta (J_{i+1,i+1+\sigma} + J_{i+1+\sigma,i+1+2\sigma} + h_{i+1+\sigma})}{\cosh \beta (J_{i+1,i+1+\sigma} + J_{i+1+\sigma,i+1+2\sigma} - h_{i+1+\sigma})} \right) \\
&\quad + \frac{1}{4\beta} \log \left(\frac{\cosh \beta (J_{i+1,i+1+\sigma} - J_{i+1+\sigma,i+1+2\sigma} + h_{i+1+\sigma})}{\cosh \beta (-J_{i+1,i+1+\sigma} + J_{i+1+\sigma,i+1+2\sigma} + h_{i+1+\sigma})} \right).
\end{aligned} \tag{9}$$

The transformation does not maintain the initial conditions and after a single iteration the initially constant exchange parameters develop random components. The field h_i on the

decimated site is shared between sites $i \pm 1$ in the new space through $H_{i\pm1,\pm1}$ and $J'_{i-1,i+1}$ which introduces correlations between fields: $\overline{h'_{i-1}h'_{i+1}} \neq 0$ and between the new bonds and fields: $\overline{h'_{i-1}J'_{i-1,i+1}h'_{i+1}} \neq 0$ [31, 32], and which an exact solution must take into account. From an analytic point of view, keeping the correlations, the problem rapidly becomes intractable and we are forced to make some approximations.

One can see how correlations develop by expanding (9) in the limit of zero temperature and strong coupling constant $T \ll |h_i| \ll J_{i,j} = J$, which corresponds to rescaling near the zero-temperature sink O shown in figure 1. Rescaling by a factor of b involves replacing an element of volume b^d by a single point in a renormalized space. Under these conditions the spins within the volume element are rigidly aligned and the rescaled field variance must be given simply by fluctuations of the random field within the volume element, $h' = b^{d/2}h$. In our case ($b = 2$, $d = 1$) the random fields $h_i, h_{i+2} \ldots$ from the decimated spins are shared between two different sites ($i - 1$ and $i + 1$, $i + 1$ and $i + 3 \ldots$). The new fields are of the form $h'_{i+1} = h_{i+1} + (h_i + h_{i+2})/2$ but with correlations between fields $h'_{i\pm1}$ on adjacent sites. If the correlations that develop on rescaling are neglected, the field variance for the rescaled element is given by $h' = \sqrt{3/2}h$: less than the value $\sqrt{2}h$ imposed by dimensionality. That is, without these correlations the fluctuations of the random field are smoothed over and their effect is implicitly underestimated. We propose taking the correlations into account in a phenomenological manner by replacing $H_{i+1,-1} + H_{i+1,+1}$ in equation (9) by $2H_{i+1,-1}$, as shown in figure 2, whereby h'_{i+1} depends on h_i and h_{i+1} but no longer depends on h_{i+2}. If the fields are repartitioned as proposed above, one immediately finds an upper bound for the renormalized field, $h'_{i+1} = h_{i+1} + h_i$, which gives the correct field variance $h' = \sqrt{2}h$.

Returning to the full problem, with couplings and random field, we make a further approximation of replacing $J_{i,j}$ on the right-hand side of equation (9) by the first moment of the distribution $J = \overline{J_{i,j}}$ evaluated at the previous iteration. This series of approximations is best tested *a posteriori*, however, we remark here that this approximation does not decouple the ferromagnetism from the disorder: rather there remains a strong interaction between the two sets of parameters through the equations for J' and $H_{i,\sigma}$. Several groups have followed the development of the distribution of coupling constants using stochastic Migdal–Kadanoff algorithms [31, 32, 29]. They find a tail in the distribution at small $J_{i,j}$, correlated with large values of $h_i + h_j$ [31, 32]. However as our results compare favourably we conclude

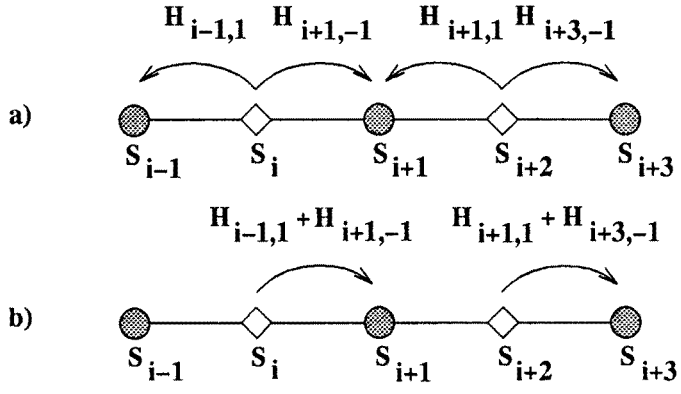

Figure 2. Field-moving approximation on the $1 - d$ chain: (a) shows the exact partition, (b) shows the approximation used in the calculation.

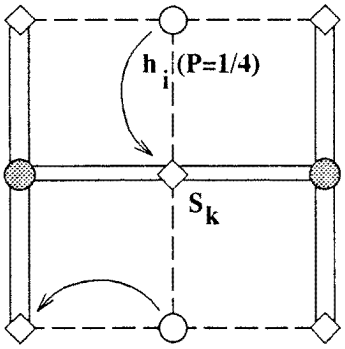

Figure 3. Symmetric Migdal–Kadanoff bond-moving scheme, in two dimensions. Bonds are displaced from the dotted to the double curves and the central spin (open circle) is decoupled. The fields h_i on the decoupled sites are placed on one of the four sites, k, with probability $P = \frac{1}{4}$.

that the main characteristics of the RFIM are given by the interaction between the mean ferromagnetic coupling and the random fields.

We move from one to higher dimensions using the Migdal–Kadanoff bond-moving algorithm [30], which is described in more detail in appendix A. Our symmetric scheme, which lends itself well to analytic work, is shown in figure 3 in two dimensions. Bonds are moved from the centre to the edges of a d-dimensional cube of side 2. What remains is a series of one-dimensional links, of bond strength $\alpha_d J$: $\alpha_d = 2^{d-1}$, which can be decimated using the one-dimensional equations, once the random fields have been correctly dealt with.

In two dimensions the procedure leaves a random field stranded on the decoupled spin in the centre of the cell. In the renormalization all 2^d field elements must contribute to the single point in the new space and so the stranded field must be repartitioned onto the neighbouring participating sites. How this repartition is done is rather arbitrary.

One possibility, which has been used in the renormalization of the XY model in the presence of crystal fields [33] and in numerical renormalization of the RFIM [29], is to divide the central field, h_i, equally between the k nearest-neighbour sites. However, this field partitioning again leads to correlations between fields on renormalized sites, which if neglected would lead to a smoothing over the random-field fluctuations. In this case the total field on one of the k sites would be $h_k^* = h_k + (h_{i1} + h_{i2})/4$, where h_{i1} and h_{i2} are the stranded fields from two neighbouring cells. As in one dimension, if we consider dimensional arguments for the random fields, valid near the zero-temperature sink O, we find a field variance on the site k $h^{*2} = 9/8h^2$. Each cell effectively contains two sites of type k plus a corner site (see appendix B), which gives a total field variance for a point in the renormalized space $h' = \sqrt{13}/2h$, while dimensional analysis demands that the upper bound is $h' = 2h$.

We propose an alternative partition scheme that preserves this upper bound for h': rather than divide the field into equal parts, we place the entire field on any one of the nearest-neighbour sites with probability $p_k = 1/k = \frac{1}{4}$, as shown in figure 3. As the fields are not divided up, no correlations develop between spins on neighbouring sites. In the two-dimensional example under consideration, as the site k can receive a field from either of the two cells the total field h_k^* is either the original field only, the sum of two fields, or of three fields, with probabilities $P = \frac{9}{16}$, $\frac{3}{8}$, or $\frac{1}{16}$ respectively. The variance of the distribution for the field on site k is therefore $(h^*)^2 = 3/2h^2$. This gives the total field variance $h'^2 = h^2 + 2(h^*)^2 = 4h^2$ as required.

The procedure also works in three dimensions. Here there are stranded fields at the centre of the cubic cell and in the centre of the cube faces (see appendix B). Moving the central field to one of the faces and then the fields from the faces to the sites to be decimated,

which are on the edges of the cube, one finds $(h^*)^2 = 7/3h^2$. This is a tedious calculation and rather than go into details, in the appendices we present a formal generalization to d-dimensions which yields the result:

$$(h^*)^2 = \frac{2^d - 1}{d} h^2. \tag{10}$$

Our new partitioning might be called a random-phase approximation, compared with the mean-field approximation proposed in [33]. Both work equally well for non-disordered systems as they satisfy a minimum requirement of contributing 2^d field terms for the new point in the renormalized space. We emphasize, however, that with our choice for the field partitioning our calculation takes into account the random-field fluctuations correctly, without the need to follow the development of complicated correlations. With it we predict $d_l = 2$, in agreement with Imry–Ma arguments. For any field partition that underestimates the random-field fluctuations, while at the same time neglecting the induced correlations between fields and coupling constants one finds $1 < d_l < 2$.

This is a general result: smoothing over the field fluctuations gives $h' = 2^{d/2-\sigma}h$, $\sigma > 0$, [16], even for the above dimensional analysis. In the pure system we have $J' = 2^{d-1}J$† which, at d_l, is put equal to the field term in the Imry–Ma argument. If $\sigma > 0$, as in the mean field distribution [33], we find $d_l < 2$. One can in fact work backwards, imposing Imry–Ma at the outset and arriving at equation (10) in the approximation where the $J_{i,j}$ are constant.

We are now finally in a position to apply the bond-moving scheme: we replace J by $\alpha_d J$, $\alpha_d = 2^{d-1}$, on the right-hand side of equations (9). We then average the terms involving J and h_i over a field distribution with variance h^*. Our d-dimensional decimation equations read

$$\begin{aligned}
J' &= \frac{1}{2\beta}\int_{-\infty}^{\infty} \mathrm{d}t\ P(t) \log \frac{\cosh\beta(2\alpha_d J + t)}{\cosh\beta t} \\
h'^2 &= h^2 + \frac{d}{4\beta^2}\int_{-\infty}^{\infty} \mathrm{d}t\ P(t) \log^2 \frac{\cosh\beta(2\alpha_d J + t)}{\cosh\beta(2\alpha_d J - t)} \\
h_0' &= h_0 + \frac{d}{2\beta}\int_{-\infty}^{\infty} \mathrm{d}t\ P(t) \log \frac{\cosh\beta(2\alpha_d J + t)}{\cosh\beta(2\alpha_d J - t)} \\
P(t) &= \frac{1}{\sqrt{2\pi}h^*} \exp -\frac{(t - h_0^*)^2}{2h^{*2}} \qquad h_0^* = \frac{2^d - 1}{d} h_0.
\end{aligned} \tag{11}$$

The renormalization flows given by equation (11), in three dimensions, are shown in figure 4. The zero-field fixed point is unstable to disorder and the ferromagnetic and paramagnetic phases are separated by a critical line, with all trajectories near the phase boundary flowing towards the zero-temperature fixed point. The value ω_c and the critical exponents can be found by expanding the equations (11) at $T = 0$.

† Note that $d-1$ is the value of y close to the zero-temperature sink of the pure system. Near the zero-temperature fixed point the dimensional analysis gives $y = d/2$ (see section 4). This is due to a duality transformation between h and J as $T \to 0$.

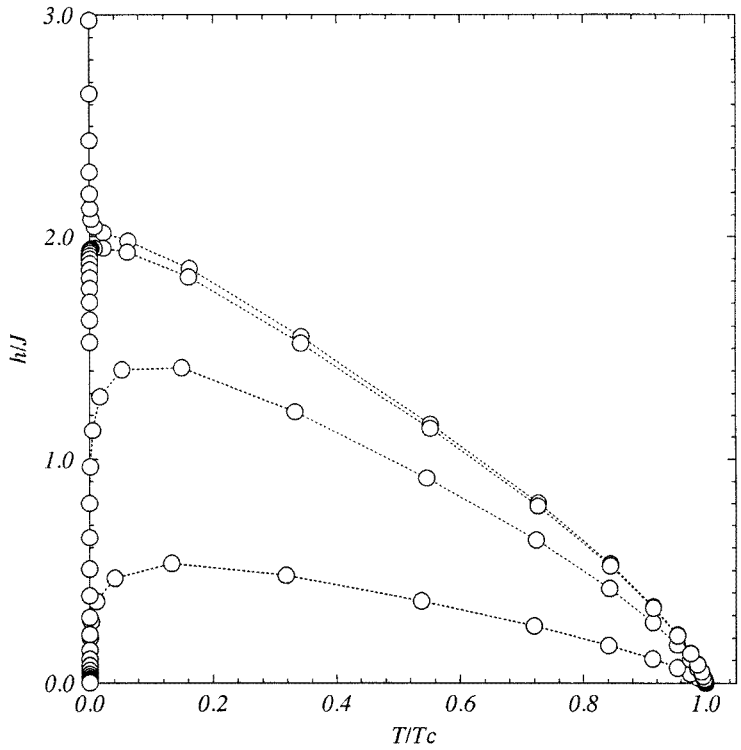

Figure 4. Flow diagram, in three dimensions using equations (11). The open circles give the values of the parameters on successive applications. The dotted curves are a guide to the eye.

After some tedious manipulation we find

$$
\begin{aligned}
&J' = \alpha_d J \phi(\omega^*/\sqrt{2}\alpha_d) \\
&\omega'^2 J'^2/J^2 = \omega^2\{1 + (2^d - 1)\mathrm{erf}(\alpha_d\sqrt{2}/\omega^*)\} + 4d\alpha_d^2\{1 - \mathrm{erf}(\alpha_d\sqrt{2}/\omega^*)\} \\
&\qquad\qquad -2\sqrt{\frac{2}{\pi}}d\alpha_d\omega^* \exp\left(-\frac{2\alpha_d^2}{\omega^{*2}}\right) \qquad (12) \\
&h_0' = h_0\{1 + (2^d - 1)\mathrm{erf}(\alpha_d\sqrt{2}/\omega^*)\} \\
&\phi(x) = 2\int_0^{1/x} \frac{\mathrm{d}t}{\sqrt{\pi}} \exp(-t^2)(1 - xt)
\end{aligned}
$$

where $\mathrm{erf}(x)$ is the error function and $\omega^* = h^*/J$. The function $\phi(\omega)$ is positive for $\omega \geqslant 0$, it decreases as ω increases, and is contained within the interval $[0, 1]$.

Eliminating J and J' in equations (12) and setting $\omega = \omega' = \omega_c$ we find an implicit equation for the critical field which can be solved numerically. We recuperate the correct lower critical dimension, $d_l = 2$ by setting $\omega_c = 0$. Putting equations (3) and (12) equal and linearizing with respect to h_0, $\tau = T/J$ and $\delta\omega$, whose equation takes the form

$$
\begin{aligned}
2\alpha_d^2\omega_c\phi_c^2\delta\omega' = \Bigg\{ &-\sqrt{2}p\alpha_d\omega_c^2\phi_c\phi_c' - \frac{4}{\sqrt{\pi}}\sqrt{2}dp\alpha_d \exp\left(-\frac{2\alpha_d^2}{p^2\omega_c^2}\right) \\
&+ 2\omega_c\left[1 + dp^2\mathrm{erf}\left(\frac{\sqrt{2}\alpha_d}{p\omega_c}\right)\right]\Bigg\}\delta\omega \qquad (13)
\end{aligned}
$$

we solve numerically for x, y, z in d dimensions. Near the trivial fixed point O, our scheme reproduces the correct limiting values, $x \to d$, $y \to d-1$ as well as the correct scaling of the random fields discussed in detail above.

3. Results in three dimensions

In three dimensions we find $\omega_c = 1.956$, and using the scaling relations for the RFIM, which can be derived from (4) [24]

$$\begin{aligned} &\nu = 1/z \qquad 2-\alpha = (d-y)\nu \qquad \beta = \nu(d-x) \\ &\gamma = (2x-y-d)\nu \qquad \delta = (x-y)/(d-x) \\ &\eta = d+2+y-2x \qquad \overline{\eta} = d+4-2x. \end{aligned} \tag{14}$$

We find the following complete set of exponents in three dimensions

$$\begin{aligned} &x = 2.991 \qquad y = 1.491 \qquad z = 0.449 \qquad \nu = 2.23 \\ &\alpha = -1.360 \qquad \beta = 0.02 \qquad \gamma = 3.318 \qquad \delta = 167 \\ &\eta = 0.510 \qquad \overline{\eta} = 1.019 \qquad \overline{\eta} - 2\eta = -0.002 \end{aligned} \tag{15}$$

which can be compared, in table 1, with other values found in the literature.

Our results are in very close agreement with stochastic Migdal–Kadanoff renormalization results [31, 32, 29]. The values of η and $\overline{\eta}$ quoted are the same as ours within their numerical errors, as are the values of ν, α and β found in [31, 32]. The numerical values of Berker *et al* [31, 32] are particularly precise and our agreement with their results is so good as to suggest that the details of the methods are related. In appendix A we discuss the various Migdal–Kadanoff schemes and the problems that field terms present. We conclude that our bond- and field-moving procedures are the correct logical steps that map the RFIM from the cubic lattice to the hierarchical necklace lattice used for the renormalization in [31, 32]. Further, the excellent agreement justifies the approximation shown in figure 2, to deal with the correlations that develop between the random fields on renormalization, at least within the Migdal–Kadanoff approximation. We can therefore expect that our analytic technique will incur errors characteristic of the Migdal–Kadanoff method but will not lead to inconsistences over and above this.

There is almost universal agreement in the literature on the values of η, $\overline{\eta}$ and β. In Monte Carlo simulation on the RFIM [21] one finds $\eta = 0.56 \pm 0.03$, $\overline{\eta} = 1.00 \pm 0.06$, $\beta = 0$, while simulations on a diluted antiferromagent in the presence of a constant magnetic field

Table 1. Estimates of the critical exponents of the RFIM.

Reference	η	$\overline{\eta}$	ν	β	α	γ
Present work	0.510	1.019	2.23	0.02	−1.360	3.318
[31]	0.51	1.02	2.25	0.02	−1.37	
[32]	0.51	1.02	2.25 ± 0.01	0.02 ± 0.0005	−1.39 ± 0.016	
[29]	0.56	1.0				2.1 ±0.2
[21, 35]	0.56 ± 0.03	1.0 ± 0.06	1.6 ± 0.3	0.0 ± 0.05	−1.0 ± 0.3	2.3 ± 0.3
[14]	0.5	1.0	1.3	0		2.0 ± 0.5
[34]		1.1		0.05		
[28]						2.1 ± 0.2
[15]	0.25					1.31, 1.75
[36]					-1.0	

[14] yield $\eta \approx 0.5, \overline{\eta} \approx 1.0, \beta \approx 0$. Finally, from exact ground-state calculations Ogielski [34] predicted $\overline{\eta} = 1.1, \beta = 0.05$. The experimental evidence could point towards a smaller value of η: for example Belanger *et al* [15] would find a value of $\eta \approx 0.25$ by using the scaling relations, however, the errors on the measurements are large.

The reason why these exponents are all so similar despite widely ranging techniques and approximations is that the deviation from the values given by simple dimensional arguments is small. Dimensional arguments give the bounds $x \leqslant d$, $y \leqslant d/2$ and $z \leqslant d/2 - 1$ (see section 4). If the deviation from these bounds is really so small, then any correctly implemented procedure should give accurate results. We find that the deviation is particularly small for x and to a lesser extent for y. Judging from the literature this appears to be universally true and with four different procedures giving similar small values for the magnetization exponent we begin to get an established picture of the random field disorder driving the transition to the limit of being first order.

There is much more variation in the literature for the exponents that depend principally on the third eigenvalue z, namely ν, α and γ. Experimentally $\nu \approx 1.0$ [15]. Our calculation predicts $\nu \approx 2.25$, while Monte Carlo predicts $\nu = 1.6 \pm 0.3$ [35] and $\nu = 1.3$ [14] and the optimization scheme of Ogielski $\nu = 1.0$. It is typical of the Migdal–Kadanoff approximation that it overestimates the value of ν: for example in a pure three-dimensional Ising model one finds $\nu = 1.064$ compared with the experimental result of $\nu = 0.64$. We can therefore be confident in assuming that our value is too large. In fact, if the true value is less that 2 it would mean that z is greater than the dimensional result $z = d/2 - 1$ which would be in contrast to that which we find from the ϵ expansion in section 4.

The large value of ν gives us a large value of γ and a strongly negative value of α. Other values of γ are experimental: $\gamma = 1.31 \pm 0.03$ and 1.75 ± 0.2 [15], numerical: 2.0 ± 0.5 [14] and 2.3 ± 0.3 [35], 2.0 from the Casher–Schwartz renormalization scheme [29] and 2.1 ± 0.2 [28] from series expansions. The largest variations come in the values of α, here the predicted values vary in sign which completely changes the observable physical phenomenon the exponent describes. Ogielski [34] predicted a positive value, while Monte Carlo gives $\alpha \leqslant 0$ [14] and $\alpha = -1.0 \pm 0.3$ [35]. Experimental results do not show a divergence in the specific heat and the cusp observed has been fitted with $\alpha \leqslant 0$ in the case of $Fe_xZn_{1-x}F_2$ [9, 10] and $\alpha = -1.0$ for $Fe_xMg_{1-x}Br_2$ [36]. It could therefore be that the Monte Carlo simulation results are fairly close to the truth. However, as the experiments and Monte Carlo suffer from exponentially long relaxation times they might both be measuring non-equilibrium phenomena. Putting $\alpha \approx 0$ in the scaling relation, and using our value of y gives $\nu \approx \frac{4}{3}$, which is perhaps a reasonable estimate.

4. Expansion in $\epsilon = d - 2$

We gain more insight into the general trends for the exponents by expanding analytically in powers of $\epsilon = d - 2$, where to first order in ϵ we recover the analytic results of Cao and Machta [31].

$$x = d = 2 + \epsilon \qquad y = d/2 = 1 + \epsilon/2 \qquad z = d/2 - 1 = \epsilon/2. \tag{16}$$

These differ slightly from the first calculation by Bray and Moore [24], as one finds $\nu = 2/\epsilon$, compared with their value of $\nu = 1/\epsilon$. To order ϵ we therefore find $\overline{\eta} - 2\eta = 0$ and two independent parameters only.

The leading corrections to equations (16) are exponentially small in $1/\epsilon^2$ [24, 31]. To see this we first write

$$\begin{aligned}
&\operatorname{erf}\left(\frac{1}{r}\right) \simeq 1 - \frac{r}{\sqrt{\pi}} \exp\left(-\frac{1}{r^2}\right)\left[1 - \frac{r^2}{2} + \frac{3r^4}{4}\right] \\
&\phi(r) \simeq 1 - \frac{r}{\sqrt{\pi}} + \frac{r}{\sqrt{\pi}} \exp\left(-\frac{1}{r^2}\right)\left[\frac{r^2}{2} - \frac{3r^4}{4}\right] \\
&\phi'(r) = -\frac{1}{\sqrt{\pi}}\left[1 - \exp\left(-\frac{1}{r^2}\right)\right]
\end{aligned} \tag{17}$$

where

$$r \equiv \frac{p\omega_c}{\sqrt{2}\alpha_d} \ll 1 \qquad p^2 = \frac{2^d - 1}{d}. \tag{18}$$

We can calculate r as a function of ϵ using (12) and setting $\omega = \omega_c$. After some calculation we obtain

$$r = \frac{\sqrt{\pi}\log 2}{2}\epsilon + \cdots. \tag{19}$$

Putting this into (13) yields

$$\delta\omega' \simeq 2^{d/2-1}\left(1 - \frac{3}{2\sqrt{\pi}r}\exp\left(-\frac{1}{r^2}\right)\right)\delta\omega \tag{20}$$

and therefore

$$z = \frac{\epsilon}{2} - \frac{3}{\pi\epsilon\log^2 2}\exp\left(-\frac{4}{\pi\epsilon^2\log^2 2}\right) + \cdots. \tag{21}$$

Similarly, using the first of equations (12)

$$y = d - 1 + \frac{1}{\log 2}\log\phi(r). \tag{22}$$

We remark that, in the absence of random fields, we find $y = d - 1$, as one expects for a perfectly ordered pure system. However, this is not the correct result as one approaches d_l from above. As one flows along the separatrice from the thermal to the random-field fixed point there is an inversion of the roles played by h and by J: a duality $h \leftrightarrow J$ with the result that the dimensional arguments give $y = d/2$ and not $d-1$. In effect, the eigenvectors of the renormalization group applied at the thermal and random-field fixed point are related nonlinearly, which leads to this inversion [37]. Physically this inversion may come from the roughening of domain walls [38]. It is the reason why the exponent y describes how the width of the field distribution grows in stochastic Migdal–Kadanoff procedures [31].

This inversion falls out of a development of $\log(\phi)$, taking care to include subsequent terms from (19). Alternatively one can expand ϕ^2 directly in (12) arriving at the result

$$y = 1 + \frac{\epsilon}{2} - \frac{3\epsilon}{8}\exp\left(-\frac{4}{\pi\epsilon^2\log^2 2}\right) + \cdots. \tag{23}$$

Similarly, using the expansion for the error function $\operatorname{erf}(1/r)$ we find

$$x = 2 + \epsilon - \frac{3\epsilon}{8}\exp\left(-\frac{4}{\pi\epsilon^2\log^2 2}\right) + \cdots. \tag{24}$$

Using the scaling relations (14) the corrected x, y, z give

$$\beta = \frac{3}{4}\exp\left(-\frac{4}{\pi\epsilon^2\log^2 2}\right) + \cdots. \tag{25}$$

However, to this order the difference $\bar{\eta} - 2\eta$ is still zero and to find the non-zero term we have to push further. We can write the expressions for x and y

$$\begin{aligned} x &= d - (1 - 2^{-d}) \frac{r}{\sqrt{\pi} \log 2} \left(1 - \frac{r^2}{2}\right) \exp\left(-\frac{1}{r^2}\right) + \cdots \\ y &= \frac{d}{2} - (1 - 2^{-d}) \frac{r}{\sqrt{\pi} \log 2} (1 - r^2) \exp\left(-\frac{1}{r^2}\right) + \cdots \end{aligned} \tag{26}$$

and after some final manipulation we arrive at the result

$$\bar{\eta} - 2\eta = -\frac{3\pi\epsilon^3 \log^2 2}{32} \exp\left(-\frac{4}{\pi\epsilon^2 \log^2 2}\right). \tag{27}$$

These analytic results confirm the consistently small values in the literature. Dimensional analysis predicts $\beta = 0$, $\bar{\eta} - 2\eta$ and so two independent exponents only. We find corrections to this analysis, which are exponentially small in ϵ. As discussed in the previous section, this appears to be a reasonable representation of the truth for the eigenvalues x and y, but there is experimental, theoretical and numerical evidence to suggest that the variation is much bigger for the eigenvalue z. Further, the deviation, $z > \epsilon/2$, appears to be in disagreement with equation (21).

All numerical work gives the Schwartz–Soffer inequality satisfied as an equality [31, 29, 28, 21] within the numerical errors and from series expansions one finds $2\eta = \bar{\eta}$ in $d = 3$, $d = 4$ and $d = 5$ [28]. This is in disagreement with the replica calculation in [27], where a solution with $\bar{\eta} - 2\eta < 0$ is predicted with values lying in a narrow range close to zero. In our scheme, which does not suffer from statistical error, we are able to quantify the inequality. With this exponential dependence, our results are consistent with both the high-precision series expansion, and the replica calculation, although we remark also that we may simply have a measure of the extent to which the Migdal–Kadanoff approximation fails.

In figure 5 we show η and $\bar{\eta}$, together with $\bar{\eta} - 2\eta$ versus d, calculated numerically using the procedure outlined in section 3. In contrast to the series expansion, the difference, $\bar{\eta} - 2\eta$, begins to grow between $d = 3$ and 4. This could indicate a continuous development towards the 'dimensional reduction' result $\bar{\eta} = \eta$ at $d = 6$ [27]. However η and $\bar{\eta}$ do not fall smoothly towards zero as one approaches $d = 6$, rather they reach minimum values between $d = 4$ and $d = 5$. This indicates the breakdown of the Migdal–Kadanoff scheme at higher dimension, as one might expect from results on the pure system.

5. Crossover from pure to random-field behaviour

The RFIM is subject to the phenomenon of crossover as the random-field variance h is a relevant variable at the critical point of the pure system [39]: take a renormalization flow in the dimensionless parameters τ and ω starting close to the thermal critical point τ_C. The small parameters are $t = (\tau - \tau_C)/$ and ω^2, with $\omega^2 \ll |t|$. With these starting conditions the disorder has little effect at small length scales and the system behaves as in zero field. As it is relevant, ω grows with changing length scale and when the two parameters are of the same order of magnitude the behaviour changes rapidly to that of the random-field fixed point at $\tau = 0$. This can be seen qualitatively in figure 4 by considering the flows close to the separatrice joining the two fixed points. The points represent the evolution after repeated rescaling by $b = 2$. One can see that the evolution between the two asymptotic regions occurs in just a few iterations. This abrupt change is the crossover effect which occurs at a well-defined length scale ξ_d.

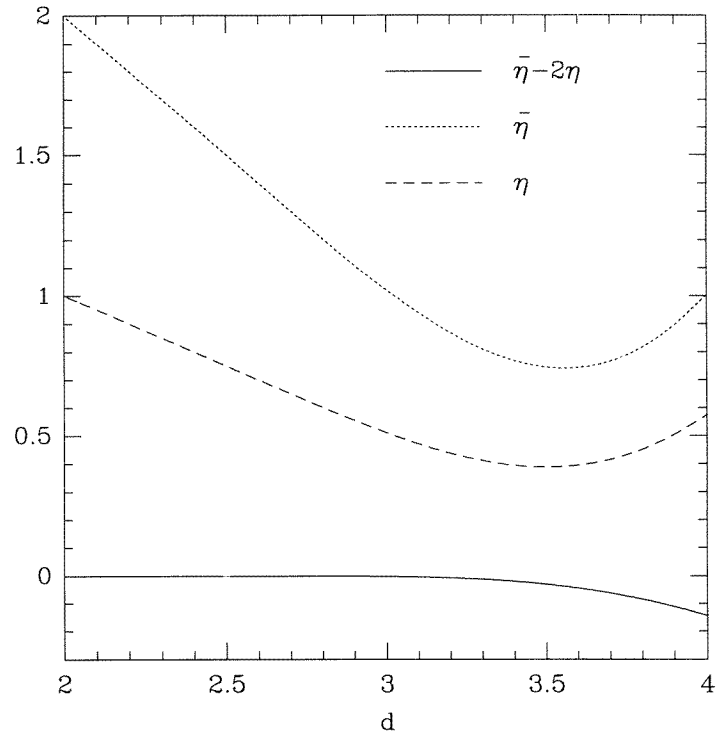

Figure 5. Exponents η, $\bar{\eta}$ and the difference $\bar{\eta} - 2\eta$ against dimension d.

A crossover exponent can be calculated from the application of the linearized renormalization group on the two-dimensional space of variables $\mu = (\tau, \omega^2)$ near to the thermal critical point

$$\delta\mu' = R_b^L \delta\mu. \tag{28}$$

R_b^L can be calculated from equations (11). It is directly diagonalized by variables t and ω^2, with orthogonal eigenvectors e_τ and e_{ω^2} along and perpendicular to the temperature axis of the phase diagram. Equation (28) can then be written

$$\begin{aligned}\delta\mu' &= tb^{y_\tau} e_\tau + \omega^2 b^{y_{\omega^2}} e_{\omega^2} \\ &= tb^{y_\tau}\left(e_\tau + \frac{\omega^2}{t} b^{y_{\omega^2}-y_\tau} e_{\omega^2}\right)\end{aligned} \tag{29}$$

where y_τ and y_{ω^2} are the two independent exponents. Fixing $tb^{y_\tau} = 1$ we finally write

$$\delta\mu' = e_\tau + \omega^2/t^{y_{\omega^2}/y_\tau} e_{\omega^2} \tag{30}$$

from which we define the crossover exponent $\phi \equiv y_{\omega^2}/y_\tau$. The effect of the disorder is contained in the term $\omega^2/|t|^\phi$. If it is small, thermal fluctuations dominate while when large the disorder dominates. The singular part of the free energy will therefore have the form [2, 40, 41]

$$F(t, \omega^2) = |t|^{2-\alpha} g(\omega^2/|t|^\phi). \tag{31}$$

It has been shown, for the RFIM, where along the temperature axis there is no disorder that ϕ should be equal to the susceptibility exponent, γ_0, for the pure system [40, 41].

Dimensional arguments give for both exponents

$$\gamma_0, \phi \leqslant \frac{d}{d-1}. \tag{32}$$

The equality does not necessarily hold for the diluted antiferromagnet, as the dilution results in disorder, even at zero field, leading to the inequality [41]

$$\phi \geqslant \gamma_0. \tag{33}$$

Linearizing equations (11) we find

$$\begin{aligned} \delta\tau' &= \alpha_d \tanh\left(\frac{2\alpha_d}{\tau_c}\right)\delta\tau \\ \omega'^2 &= \left\{1 + (2^d - 1)\tanh^2\left(\frac{2\alpha_d}{\tau_c}\right)\right\}\omega^2 \end{aligned} \tag{34}$$

from which we deduce

$$\phi = \frac{y_{\omega^2}}{y_\tau} = \frac{\log\{1 + (2^d - 1)\tanh^2(2\alpha_d/\tau_c)\}}{(d-1)\log 2 + \log\tanh(2\alpha_d/\tau_c)}. \tag{35}$$

We need a second exponent for the pure system in order to calculate γ_0. We can calculate y_{h_0}, the exponent giving the renormalization of the magnetic field, from the third of equations (11) with $h = 0$:

$$y_{h_0} = \frac{1}{\log 2}\log\{1 + (2^d - 1)\tanh(2\alpha_d/\tau_c)\} \tag{36}$$

from which, using the scaling relations for the pure system we find

$$\gamma_0 = \frac{2y_{h_0} - d}{y_\tau} \tag{37}$$

and finally

$$\frac{\phi}{\gamma_0} = \frac{\log\{1 + (2^d - 1)\tanh^2(2\alpha_d/\tau_c)\}}{2\log\{1 + (2^d - 1)\tanh(2\alpha_d/\tau_c)\} - d\log 2}. \tag{38}$$

In three dimensions we find $\phi/\gamma_0 = 1.1$ with $\phi = 1.473$ and $\gamma_0 = 1.326$ which compares remarkably well with experimental values [2] $\phi/\gamma = 1.1$, with $\phi = 1.42 \pm 0.02$ and $\gamma_0 = 1.31 \pm 0.03$ (see also [9]: $\phi = 1.40 \pm 0.05$). Such good quantitative agreement is clearly rather fortuitous as the Migdal–Kadanoff procedure is known to be of limited accuracy in its predictions for the pure system. For example developments in $\epsilon = 4 - d$ give $\gamma_0 = 1.241 \pm 0.004$ [42]. However, these characteristic errors should cancel in the ratio, making the predictions for ϕ/γ more reliable. One should also note that, as real systems remain ergodic up to the crossover to random-field critical behaviour, then ϕ is the exponent characteristic of the RFIM which can be measured with the most confidence.

In figure 6 we show the evolution of the ratio with dimension. We see that inequality (33) is satisfied for all dimensions, with the deviation from the equality growing rapidly as one exceeds $d = 2$. We can quantify this deviation by developing equation (38) in $\epsilon = d - 1$. Correction terms are exponentially small in $1/\epsilon$

$$\frac{\phi}{\gamma_0} = 1 + \frac{1}{\log 2}\exp(-4/\epsilon) + \frac{2}{\log^2 2}\exp(-6/\epsilon) + \cdots. \tag{39}$$

We therefore have, rather unexpectedly, a result that is consistent with the diluted antiferromagnet rather than our starting model, the RFIM. It is possible that the modification occurs when displacing fields $H_{i-1,1}$ at the one-dimensional stage of the rescaling process.

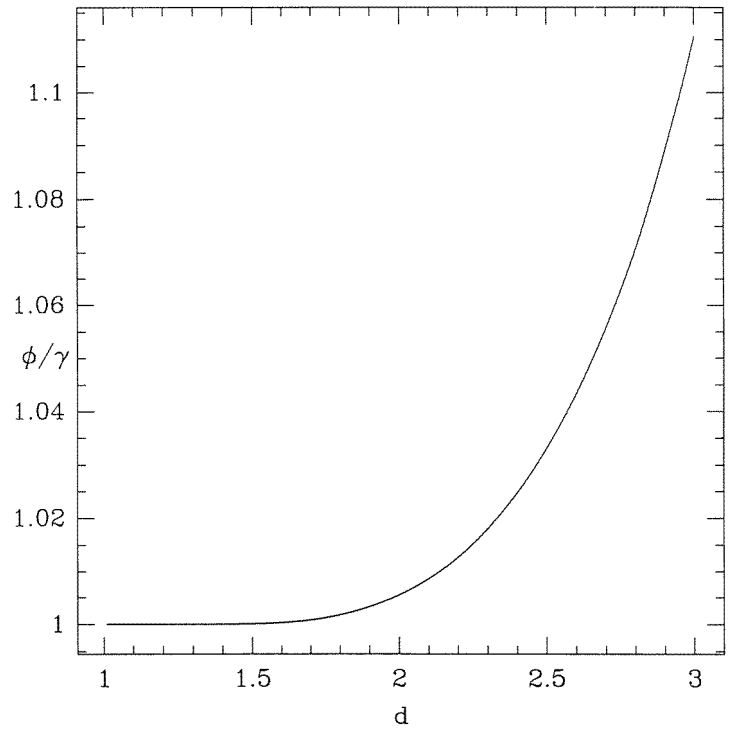

Figure 6. Evolution of the ratio ϕ/γ_0 versus dimension d.

This step mixes bonds and random fields in an approximate manner, compared with the exact decimation and must introduce an implicit random bond term even in the limit of the field strength going to zero. It would be interesting to investigate this point further.

6. Discussion

The scaling relations (14) are equivalent to those of a pure system with $d' = d - y$, plus a supplementary relation $\overline{\eta} = \eta + 2 - y$. It has therefore been proposed that dimensional reduction should be modified in the light of this third exponent [23, 24] and that one could find the exponents of a pure Ising model in dimension $d' = d - y$. There is no proof of this, that is there is no *a priori* reason why the universality class of the reduced system in dimension d' should be that of the Ising model.

In the absence of a proof, our calculation allows us to test the modified dimensional reduction systematically in powers of ϵ and it is easily shown to hold to first order: in dimension d' the exponent ν_0 for the pure Ising system is defined by the transformation

$$|t'| \sim b^{1/\nu_0}|t| \qquad t = (T - T_C)/T_C \tag{40}$$

with $1/\nu_0 \approx d' - 1$ as one approaches the lower critical dimension. Defining $d' = d - y = 2 + \epsilon - (1 + \epsilon/2) = 1 + \epsilon/2$ we find $\nu_0 = 2/\epsilon$, in agreement with (16). A second exponent can be calculated to the same order by, for example, using the scaling relations (14) and the values (16) from which we find $\gamma_0 = d'/(d' - 1)$ which corresponds to the Ising exponent in dimension d' to this order of approximation (see equation (32)).

One could test to higher order in ϵ, within the Migdal–Kadanoff procedure, by solving the equations for the pure system in dimension d'

$$\begin{aligned} t' &= \alpha_{d'} \tanh(2\alpha_{d'} K_c) t \\ K_c &= \tfrac{1}{2} \log \tanh(2\alpha_{d'} K_c) \end{aligned} \tag{41}$$

with $d' = 1 + \epsilon/2 + \mathrm{O}(\exp(-1/\epsilon^2))$ defined from equation (23) for y.

Recently Jolicoeur and Le Guillou [43] applied an extrapolation of the exponents of the pure model between the critical dimensions 1 and 4 to a reduced dimension in the range $d' \sim 1.5$, corresponding to the consensus in the literature giving $y \approx d/2$. They find that the ensemble of exponents quoted in the literature are well represented by their predictions. All of this points to the fact that modified dimensional reduction may rigorously hold. In this case, the only unknown parameter for the complete identification of the exponents for the RFIM, would be y and there is now considerable evidence to suggest that this is given to a good approximation by $y \approx d/2$. This method [43] may well therefore represent the best approximation for the exponents of the RFIM at the present time, although the agreement with Monte Carlo is based on the assumption that true equilibrium exponents were extracted from the simulations. Both experiment and simulation face the same problem, that loss of equilibrium is guaranteed as one approaches asymptotically T_C, with the result that one measures, either in equilibrium, in a subcritical regime, or non-equilibrium exponents closer to T_C [35, 44]. In either case this could lead to an under estimate for the exponent ν (see discussion in [21]). More analytical approaches are clearly needed if this point is to be clarified further.

The exponentially small corrections to the values for $x = d$, $y = d/2$, $z = d/2 - 1$ have been predicted from energetic arguments [24, 31]. In the case of a magnetic field, if all spin are parallel, the renormalized field scales as b^d and $x = d$. As one approaches d_l, ω_c approaches zero and the probability of finding a net random field large enough to turn the spins against the local magnetization direction is exponentially small in $1/\omega_c^2$. The first correction to the value of x is therefore of this order and from the analysis of section 5, it follows that $\omega_c \sim \epsilon \ldots$. Similar arguments apply for the corrections to y, but they are complicated by the fact that y approaches $d/2$ and not $d - 1$ in this limit. This duality between the magnetic coupling and the random field is possibly due to the domain wall roughening and is a key feature of the critical behaviour of the RFIM.

In the case of the eigenvalue z we again predict an exponentially small correction to the linear expression. However, as we have discussed, there is evidence in the literature to suggest that it is actually much larger and the correct behaviour for z remains an open question.

Acknowledgments

It is a pleasure to thank A Aharony, S T Bramwell, I A Campbell, M J P Gingras, J-C Le Guillou, J Kurchan and T Ziman for useful discussions.

Appendix A

In figure A1 we show the Migdal–Kadanoff [30, 33] bond-moving procedure for a square and a cubic lattice, in the absence of fields. Bonds are moved sequentially to provide a series of one-dimensional paths which can be decimated exactly. The process breaks the lattice symmetry: depending on the direction, one finds either a multiple series of 2^{d-1}

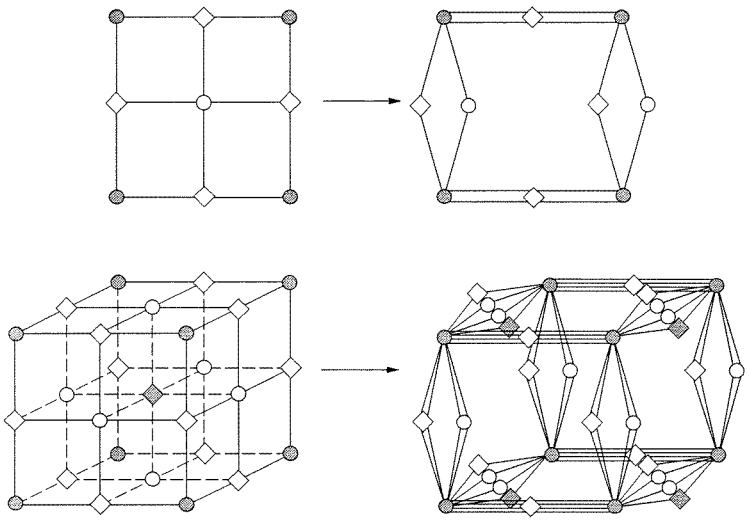

Figure A1. Migdal–Kadanoff bond-moving procedure in two and three dimensions. Single, double and quadruple lines correspond to coupling strengths of J, $2J$ and $4J$ respectively.

paths all with initial coupling strength J, a single path of strength $2^{d-1}J$, or an intermediate number of paths such that the sum of the couplings is again of order $2^{d-1}J$. Details, such as the critical temperature depend on which axis is followed in the renormalization flow, although one finds the same values for the exponents, as long as the renormalized bonds consist of 2^{d-1} contributions with strength of order J.

Renormalizing along a single direction only corresponds to renormalization on a hierarchical structure, with microscopic bond elements equal to one of the path types shown in figure A1, after the application of the bond moving scheme. Examples can be found in the literature of renormalization, either on the multiple path hierarchy [45, 47] or on the single path, of necklace hierarchy [31, 32, 46].

In the presence of field terms, however, Migdal–Kadanoff renormalization is rather an arbitrary business. A minimum condition for the renormalized cell is that it contains 2^d field contributions. This poses a problem when moving from the cubic to the hierarchical structure, as the number of sites in the renormalized cell is not conserved and renormalization takes place in a non-Euclidean space. In studies of the RFIM on the necklace hierarchy [24, 31], the correct number of random field terms is explicitly imposed for each element of the necklace. However, it is not clear how to arrive at this distribution, starting from the hypercube and making a series of field-moving steps in parallel with the bond moving shown in figure A1.

As discussed in the main text, the logical way of proceeding is a symmetric partitioning scheme [33], with the fields on displaced sites being divided into d equal parts, with one part being partitioned along each of the d-dimensions. This method seems to work satisfactorily in the absence of disorder, but in the case of the RFIM it leads to correlations between the renormalized fields [29], which cannot be treated analytically.

Our variation on the Migdal–Kadanoff renormalization scheme allows us to partition the fields analytically, even in the presence of disorder. We keep cubic symmetry by, as a first stage, moving bonds only, giving a single type of one-dimensional path in all directions and leaving a series of disconnected spins (see figure 3). As a second stage, the random

fields on the disconnected spins are partitioned using the stochastic algorithm discussed in section 2 and detailed in appendix B. Our procedure appeares to give very similar results to the numerical Migdal–Kadanoff renormalizations procedures on the hierarchical necklace [31, 32].

Appendix B

The field partition can be readily generalized to a d-dimensional network. Fundamental elements, $\mathcal{A}_d$, of this network are shown in figure B1 for $d = 1, 2, 3$. The element $\mathcal{A}_d$ can be generated from $\mathcal{A}_{d-1}$ by the application of an operator σ

$$\sigma(\mathcal{A}_{d-1}) = \mathcal{A}_d \tag{B.1}$$

which duplicates $\mathcal{A}_{d-1}$ at a distance $2a$ along the axis $\boldsymbol{x}_d$ and places new sites of varying type, s_k, midway between the original and duplicated sites. For example, the element $\mathcal{A}_1$ is constructed starting from $\mathcal{A}_0$, which is a single site of type s_0. In the centre of the line separating the two sites s_0 one finds a site of type s_1. The operation σ_2 produces $\mathcal{A}_2$ from $\mathcal{A}_1$, placing a site of type s_2 between sites of type s_1 and sites of type s_1 between the duplicated sites of type s_0. There are thus $d+1$ different site labels from s_0 on the vertices of the cell, to s_d at the centre. A site s_k can be found at the centre of the line joining two sites of type s_{k-1}.

There are $n_d(k) = 2^{d-k}C_d^k$ spins of type s_k each of which carries a combinatorial weight $1/2^{d-k}$ corresponding to the number of cells onto which it borders. For example for $d = 1$ the unit $\mathcal{A}_1$ contains one spin of type 1, with weight 1, and two spins of type 0, with weight $\frac{1}{2}$, each spin of type 0 being shared by two different segments. The total number of spins in the cell is therefore

$$n_T = \sum_{k=0}^{d} \frac{n_d(k)}{2^{d-k}} = 2^d. \tag{B.2}$$

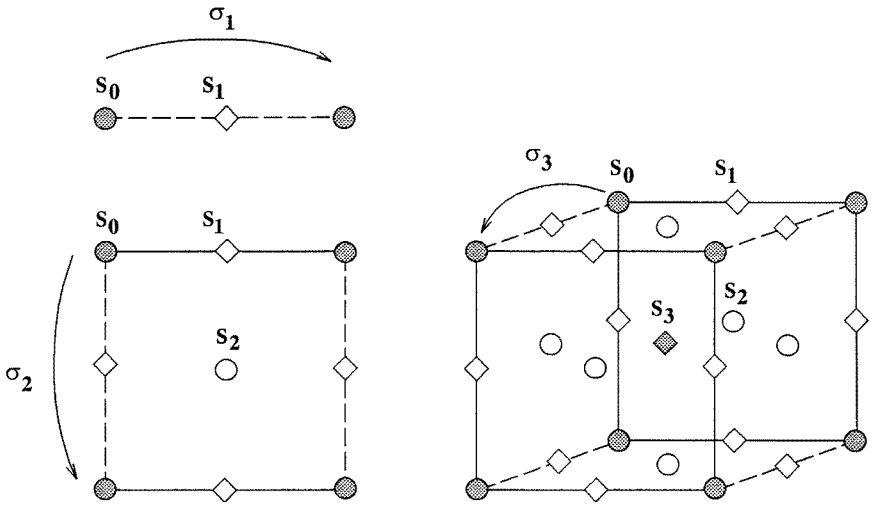

Figure B1. Construction of elements $\mathcal{A}_d$ by application of σ.

In our procedure the local fields at sites s_k, with $k = d, d-1, \ldots 2$ are successively repositioned on any one of the $2k$ sites s_{k-1} with probability

$$p_k = \frac{1}{2k} \tag{B.3}$$

until one reaches the spins s_1. The probability that the field from a site k contributes to the total field at a site s_1 is therefore

$$\alpha_k = p_k p_{k-1} \ldots p_2 .(\text{number of paths connecting } s_k \text{ to } s_1). \tag{B.4}$$

The number of paths can be calculated by considering the $(k-1)$-dimensional cube centred around s_1 with vertices s_k. For example, there are two possible ways, in any dimension, of moving from an s_3 site onto s_1 passing by one of two different s_2 sites and one possible way of passing from an s_2 site to an s_1 site. By recursion it therefore follows that there are $(k-1)!$ paths in general, from which we find

$$\alpha_k = \frac{1}{2^{k-1}k}. \tag{B.5}$$

As the random fields are uncorrelated the total field variance for an s_1 site is given by

$$h^{*2} = h^2\left(1 + \sum_{k=2}^{d} \alpha_k v_k^d(s_1)\right) \tag{B.6}$$

where $v_k^d(s_1)$ is the number of neighbours of type s_k.

To obtain a general expression for $v_k^d(s_1)$ we first define $v_k^d(s_l)$ in the interval $0 \leqslant l \leqslant k \leqslant d$ which satisfy the relations

$$v_k^d(s_l) = v_{k-1}^{d-1}(s_{l-1}) = \cdots = v_{k-l}^{d-l}(s_0). \tag{B.7}$$

The operator σ generates the recursion relation

$$v_k^{d+1}(s_0) = v_k^d(s_0) + 2v_{k-1}^d(s_0) \tag{B.8}$$

with the initial conditions $v_0^d(s_0) = 1$ and $v_1^d(s_0) = 2d$, the number of nearest neighbours in d-dimensions.

We can then solve for $v_k^d(s_0)$ by introducing the set of $(d+1)$-dimensional vectors defined by

$$\begin{aligned} &v^0 = (1, 0, \ldots, 0) \\ &\ldots \\ &v^k = (v_0^k(s_0), \ldots, v_k^k(s_0), 0, \ldots, 0) \\ &\ldots \\ &v^d = (v_0^d(s_0), \ldots, v_d^d(s_0)). \end{aligned} \tag{B.9}$$

The recursion relation can be written

$$\begin{aligned} &v^d = Rv^{d-1} = R^d v^0 \\ &R = Id + 2U \qquad U_{i,j} = \delta_{i-1,j} \qquad 1 \leqslant i, j \leqslant d+1. \end{aligned} \tag{B.10}$$

By using the property that $U^{d+1} = 0$ or by diagonalizing R, we find

$$R^d = \begin{pmatrix} v_0^d(s_0) & 0 & \ldots & \\ v_1^d(s_0) & v_0^d(s_0) & 0 & \ldots \\ \ldots & & & \\ v_d^d(s_0) & v_{d-1}^d(s_0) & \ldots & v_0^d(s_0) \end{pmatrix} \tag{B.11}$$

with elements

$$v_k^d(s_0) = 2^k C_d^k. \tag{B.12}$$

From equation (B.7) we find $v_k^d(s_1) = 2^{k-1} C_{d-1}^{k-1}$. Putting this expression into equation (B.6) and summing using the binomial relation $C_{d-1}^{k-1}/k = C_d^k/d$ we finally arrive at our desired result

$$h^{*2} = \frac{2^d - 1}{d} h^2. \tag{B.13}$$

References

[1] Nattermann T and Villain J 1988 *Phase Trans.* **11** 817
[2] Belanger D P and Young A P 1991 *J. Magn. Magn. Mater.* **100** 272
[3] Ryan D H (ed) 1992 *Recent Progress in Random Magnets* (Singapore: World Scientific)
[4] Imry Y and Ma S-K 1975 *Phys. Rev. Lett.* **35** 1399
[5] Aharony A, Imry Y and Ma S K 1976 *Phys. Rev. Lett.* **37** 1364
[6] Young A P 1977 *J. Phys. C: Solid State Phys.* **10** L257
[7] Parisi G and Sourlas N 1979 *Phys. Rev. Lett.* **43** 744
[8] Cardy J L 1984 *Phys. Rev.* B **29** 505
[9] Belanger D P, King A R, Jaccarino V and Cardy J L 1983 *Phys. Rev.* B **28** 2522
[10] Birgeneau R J *et al* 1983 *Phys. Rev.* B **27** 6747
[11] Chalker J T 1983 *J. Phys. C: Solid State Phys.* **16** 6615
[12] Fisher D S, Fröhlich J and Spencer T 1984 *J. Stat. Phys.* **34** 863
[13] Ro C, Grest G S, Soukoulis C M and Levin K 1985 *Phys. Rev.* B **31** 1682
[14] Ogielski A T and Huse D A 1986 *Phys. Rev. Lett.* **56** 1298
[15] Belanger D P, King A R and Jaccarino V 1985 *Phys. Rev. Lett.* **54** 577
Belanger D P, King A R and Jaccarino V 1986 *Phys. Rev.* B **34** 452
[16] Villain J 1984 *Phys. Rev. Lett.* **52** 1543
[17] Villain J 1985 *J. Physique* **46** 1843
[18] Fisher D S 1986 *Phys. Rev. Lett.* **56** 416
[19] Lancaster D, Marinari E and Parisi G 1995 *J. Phys. A: Math. Gen.* **28** 3959
[20] Fischer K H and Hertz J A 1991 *Spin Glasses* (Cambridge: Cambridge University Press)
[21] Rieger H 1995 *Annual Reviews of Computational Physics II* ed D Stauffer (Singapore: World Scientific) p 295
[22] Fortin J-Y and Holdsworth P C W 1996 *J. Phys. A: Math. Gen.* **29** L539
[23] Grinstein G 1976 *Phys. Rev. Lett.* **37** 944
[24] Bray A J and Moore M A 1985 *J. Phys. C: Solid State Phys.* **18** L927
[25] Wegner F J 1972 *Phys. Rev.* B **5** 4529
[26] Schwartz M and Soffer A 1985 *Phys. Rev. Lett.* **55** 2499
[27] Mézard M and Young A P 1992 *Europhys. Lett.* **18** 653
[28] Gofman M, Adler J, Aharony A, Harris A B and Schwartz M *Phys. Rev. Lett.* **71** 1569
[29] Dayan I, Schwartz M and Young A P *J. Phys. A: Math. Gen.* **26** 3093
[30] Migdal A A 1976 *Sov. Phys.–JETP* **42** 743
Kadanoff L P 1976 *Ann. Phys.* **100** 359
[31] Cao M S and Machta J 1993 *Phys. Rev.* B **48** 3177
[32] Falicov A, Berker A N and McKay S R 1995 *Phys. Rev.* B **51** 8266
[33] Jose J V, Kadanoff L P, Kirkpatrick S and Nelson D R 1977 *Phys. Rev.* B **16** 1217
[34] Ogielski A T 1986 *Phys. Rev. Lett.* **57** 1251
[35] Rieger H and Young A P 1993 *J. Phys. A: Math. Gen.* **26** 5279
[36] Karszewiski M, Kushauer J, Binek Ch, Kleeman W and Bertrand D 1994 *J. Phys.: Condens. Matter* **6** L75
[37] Berker A N and McKay S R 1986 *Phys. Rev.* B **33** 4712
[38] Binder K 1983 *Z. Phys.* B **50** 343
[39] Ma S-K 1976 *Modern Theory of Critical Phenomena* (Reading, MA: Addison-Wesley)
[40] Fishman S and Aharony A 1979 *J. Phys. C: Solid State Phys.* **12** L729
[41] Aharony A 1986 *Europhys. Lett.* **1** 617
[42] Itzykson C and Drouffe J M 1989 *Théorie Statistique des Champs* vol 1 (Editions du CNRS)

[43] Jolicoeur T and Le Guillou J-C 1997 *Preprint* ENSLAPP-A-645/97
[44] Birgenau R J, Cowley R A, Shirane G and Yoshizawa H 1985 *Phys. Rev. Lett.* **54** 2147
[45] Southern B W and Young A P 1977 *J. Phys. C: Solid State Phys.* **10** 2181
[46] Machta J and Cao M S 1992 *J. Phys. A: Math. Gen.* **25** 529
[47] Prakash S and Campbell I A 1997 *Physica* **235A** 507